AD-A119 863 AIR FORCE GEOPHYSICS LAB HANSCOM AFB MA F/G 4/2
CHANGES IN THE NATURE OF FLUCTUATIONS OF TEMPERATURE AND LIQUID--ETC(U)
MAY 82 R M DYER, I D COHEN
UNCLASSIFIED AFGL-TR-82-0147 NL

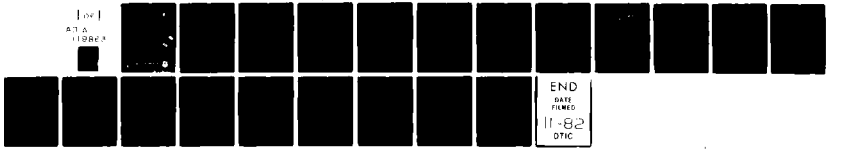

END
DATE FILMED
11-82
DTIC

AFGL-TR-82-0147
ENVIRONMENTAL RESEARCH PAPERS, NO. 777

Changes in the Nature of Fluctuations of Temperature and Liquid Water Content During the Lifetime of a Large-Scale Storm

R. M. DYER
I. D. COHEN, Capt, USAF

6 May 1982

METEOROLOGY DIVISION PROJECT 2310
AIR FORCE GEOPHYSICS LABORATORY
HANSCOM AFB, MASSACHUSETTS 01731

AIR FORCE SYSTEMS COMMAND, USAF

Unclassified

SECURITY CLASSIFICATION OF THIS PAGE (When Data Entered)

REPORT DOCUMENTATION PAGE		READ INSTRUCTIONS BEFORE COMPLETING FORM
1. REPORT NUMBER AFGL-TR-82-0147	2. GOVT ACCESSION NO. AD-A129863	3. RECIPIENT'S CATALOG NUMBER
4. TITLE (and Subtitle) CHANGES IN THE NATURE OF FLUCTUATIONS OF TEMPERATURE AND LIQUID WATER CONTENT DURING THE LIFETIME OF A LARGE-SCALE STORM		5. TYPE OF REPORT & PERIOD COVERED Scientific. Interim 6. PERFORMING ORG. REPORT NUMBER ERP No. 777
7. AUTHOR(s) R. M. Dyer I. D. Cohen, Capt., USAF		8. CONTRACT OR GRANT NUMBER(s)
9. PERFORMING ORGANIZATION NAME AND ADDRESS Air Force Geophysics Laboratory (LYC) Hanscom AFB Massachusetts 01731		10. PROGRAM ELEMENT, PROJECT, TASK AREA & WORK UNIT NUMBERS 61102F 2310G502
11. CONTROLLING OFFICE NAME AND ADDRESS Air Force Geophysics Laboratory (LYC) Hanscom AFB Massachusetts 01731		12. REPORT DATE 6 May 1982 13. NUMBER OF PAGES 21
14. MONITORING AGENCY NAME & ADDRESS(if different from Controlling Office)		15. SECURITY CLASS. (of this report) Unclassified 15a. DECLASSIFICATION/DOWNGRADING SCHEDULE

16. DISTRIBUTION STATEMENT (of this Report)

Approved for public release; distribution unlimited

17. DISTRIBUTION STATEMENT (of the abstract entered in Block 20, if different from Report)

18. SUPPLEMENTARY NOTES

19. KEY WORDS (Continue on reverse side if necessary and identify by block number)

Cloud Systems
Cloud Temperature
Cloud Liquid Water Content
Storm Development

20. ABSTRACT (Continue on reverse side if necessary and identify by block number)

The results of a spectral analysis of the horizontal fluctuations in temperature and liquid water content measured at four altitudes daily, during four days in the life cycle of a storm moving eastward across the United States, are discussed, along with a synoptic analysis of the storm. The storm itself was typical of the large-scale systems traveling across the continent during the winter season.

Each stage of the storm (development, maturity, and dissipation) exhibited distinctive spectral characteristics. In addition, the evidence is

DD FORM 1 JAN 73 1473 EDITION OF 1 NOV 65 IS OBSOLETE

Unclassified

SECURITY CLASSIFICATION OF THIS PAGE (When Data Entered)

#20 (continued)

strong that the age and previous history of the system greatly affect the fluctuation spectra.

The results of this study support the thesis of a characteristic spectral signature for cloud systems as well as for single clouds. This method may be used to determine the present growth stage of a storm system and its potential for future development.

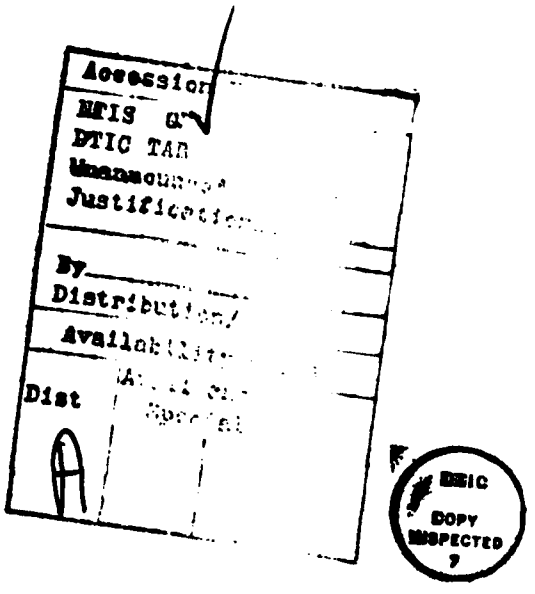

Contents

Illustrations

Illustrations

Tables

Preface

The work of the AFGL project crew, led by Major Donald Cameron, in making the measurements under trying and often hazardous circumstances, is deeply appreciated. In addition, the authors wish to thank Messrs. Terrence O'Toole, Andrew Menezes, and James Lally for the computer programming necessary in reducing and analyzing the data, and Ms. Carolyn Fadden for typing the manuscript.

Changes in the Nature of Fluctuations of Temperature and Liquid Water Content During the Lifetime of a Large-Scale Storm

1. INTRODUCTION

The existence of ordered patterns in the horizontal fluctuations of meteorological parameters in clouds has often been observed and reported. Constant altitude aircraft measurements yield preferred scale sizes, depending on the dynamic structure of the system. Ackerman[1] summarized measurements from several sources, and found one domain of preferred wavelengths to be between 200 m and 3 km. Ground-based radar measurements of clouds[2] and precipitation[3] and, less clearly, snowfall measurements at the ground,[4] reveal the same tendency toward structured, rather than random fluctuations.

Received for publication 29 April 1982

1. Ackerman, B. (1967) The nature of meteorological fluctuations in clouds, J. Appl. Meteor., 6:61-71.

2. Henrion, X., Sauvageot, H., and Ramond, D. (1978) Fine structure of precipitation and temperature in a stratocumulus cloud, J. Atmos. Sci., 35:2315-2324.

3. Foote, G. B. (1968) Variance spectrum analysis of doppler radar observations in continuous precipitation, J. Appl. Meteor., 7:459-464.

4. Dyer, R. M. (1970) Persistence in snowfall intensities measured at the ground, J. Appl. Meteor., 9:29-34.

Henrion and Sauvageot[5] have suggested that the spectral analysis of horizontal fluctuations in clouds may yield a spectral signature, varying with type of cloud. Their work was based on radar reflectivity fluctuations near the top of stratiform clouds, which they ascribed to turbulent convection.

Past observations do not demonstrate whether the spectrum of these fluctuations, Henrion and Sauvageot's spectral signature, varies with depth within the cloud or with age of the cloud system.

This paper presents the results of a spectral analysis of the horizontal fluctuations in liquid water content and temperature measured at four pressure altitudes daily, during a four-day period in the life cycle of a storm moving eastward across the United States. The results support the thesis advanced by Henrion and Sauvageot, and clearly indicate the feasibility of extending the concept from single clouds to cloud systems. Further, the results demonstrate the importance of age and previous history of the storm as factors modifying the fluctuation spectrum.

2. SYNOPTIC SITUATION – 23-27 March 1978

The storm of 23-27 March 1978 formed in Oklahoma when a wave developed on a stationary front. It deepened into an open wave and eventually became an occluded system. Figure 1 shows the track of the main low-pressure center from Oklahoma to Ohio. It also shows the fronts most closely associated with the low, and the sampling areas used for data collection.

The low center formed on the morning of the 23rd of March in central Oklahoma. By the time of the first flight (23 March 1925Z to 24 March 0136Z), the low was in southeastern Oklahoma, and was associated with an open wave system. A 500 mb trough over western Texas gave upper air support to the surface storm. At 00Z on 24 March, thunderstorms were reported along the front at McAllister and Ardmore, Oklahoma. Rain was reported throughout most of Oklahoma, southern Kansas, and the Texas panhandle, with snow being reported in northern and western Kansas. Surface temperatures in both sampling areas were about +7° C. Surface temperatures south of the front were about +20° C. Thus, the first flight looked at a small storm with great potential to develop.

The system deepened, and at the time of the second flight (24 March 1740Z to 2340Z), the low center was in eastern Missouri. There was a 500 mbar cutoff low in western Missouri, and strong southerly flow at low levels throughout the atmosphere. Rain, snow, and freezing rain fell throughout Missouri, Illinois,

5. Henrion, X., and Sauvageot, H. (1977) Spectral analysis of stratiform cloud radar observations. Geophys. Res. Lettrs., 4:360-362.

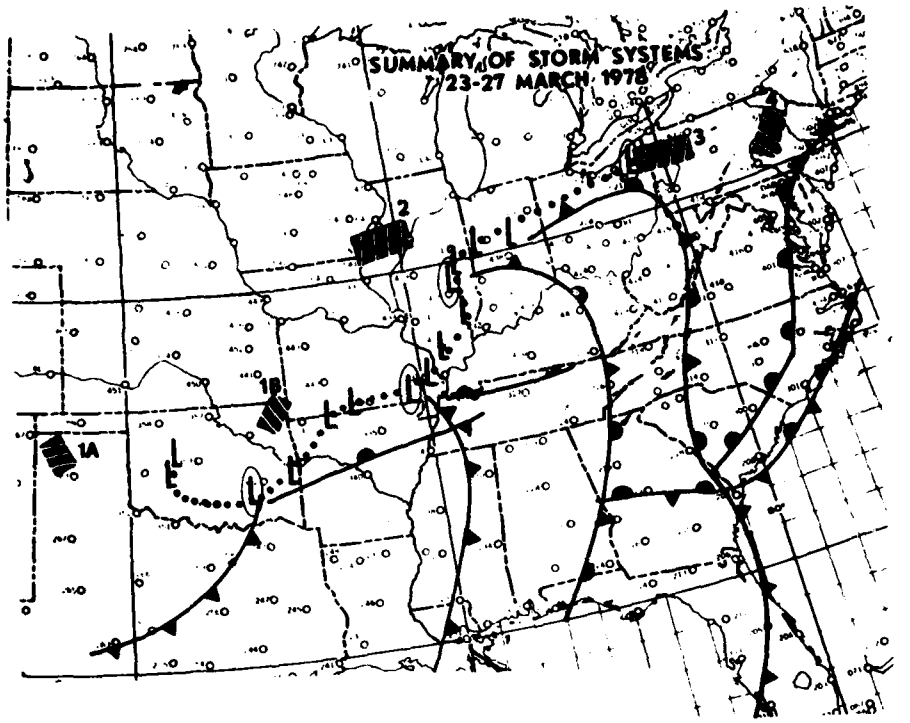

Figure 1. Track of the Main Low-Pressure Area and Frontal Systems from 23-27 March 1978. Frontal positions are those at 0000Z on 24, 25, 26, and 27 March. The positions of the low that correspond to these times are circled. The position of the low center is shown for 6-hour intervals beginning at 1200Z on 23 March. The dotted line shows the track of the low. Shaded areas indicate the sampling locations

and southern Iowa. The sampling occurred in the northern part of the precipitation shield. Stations in or near the sampling area were reporting snow or sleet. Just south of the sampling area, several stations experienced freezing rain. No thunderstorms were reported in the area. The convective activity that had been present the previous day had diminished. Surface temperatures in the sampling area were approximately -2° C.

The system began to occlude at 0300Z 25 March. As time passed, the occlusion became deeper, until by the time of the third flight (1705-2101Z) on 25 March, an

occluded front stretched from the original low, now in eastern Illinois, to another low in eastern Tennessee. By 0000Z, the occlusion stretched to Georgia. Rain was falling throughout the east coast from Maryland southward. Snow and freezing rain extended throughout Pennsylvania and southwestern New York State. Stations in the sampling area reported freezing rain and freezing drizzle. Surface temperatures were about -1° C.

The fourth flight occurred at 1444-1923Z on 26 March. The occlusion extended from Indiana to South Carolina, but a warm front that extended northward along the coast had become the dominant feature. The deep cutoff low at 500 mb provided ample warm advection along the coast. As a result, thick cloudiness covered the entire coastal plain from the Carolinas to New England. The sampling area was about 90 km ahead of the front. Stations in the area were all reporting rain with temperatures of about +2° C. Warm air aloft had penetrated well into New York State; Binghamton and Buffalo, New York had freezing rain. Farther south, several stations reported moderate rain. No convective weather was reported near the sampling area, although some rainshowers were reported in western Pennsylvania.

On 27 March, the storm moved eastward and dissipated. A flight had been planned for 27 March, but it was cancelled since the storm was no longer providing sufficient cloudiness.

The series of four flights provide a cross section of clouds in the northeast quadrant of the storm. They trace the development of the storm from a small, predominantly convective system to a large, complex, stratified occluded system.

3. C-130 INSTRUMENTATION

A. Temperature

Temperature was measured by a Rosemount Total Temperature system. The system provides a temperature with an accuracy of about ±.1° C. Although some question has arisen as to whether the system is accurate when passing between clouds and cloudless conditions, the relative temperatures within a cloud are believed to be consistent. This system (Rosemount Total Temperature Probe, Model 102CA2W) is the same as the one used on United States Air Force Weather Reconnaissance aircraft.

B. Particle Size Distributions and Liquid Water Content

Particle size distributions were determined by axial scattering, cloud, and precipitation probes manufactured by Particle Measuring Systems (PMS), Inc.

of Boulder, Colorado. Knollenberg[6] describes their operation. When many particles larger than 50 μm in length are present, the scattering probe tends to overestimate the number of particles; therefore, its data were not used for any computations in this study. Particles of sizes from 30 μm to 4500 μm were counted by the PMS 1-D cloud and precipitation probes. Particles in this range make the most significant contribution to the liquid water content of the clouds examined in this study.

The liquid water content data used in this discussion were computed from the particle size distributions obtained from the 1-D cloud and precipitation probes. Particle shapes were determined by examining shadow graphs obtained from the PMS 2-D probes. All particles in a given sample were considered to have the predominant shape or habit. For each shape, the liquid water content was represented as a function of diameter and, using this representation, the liquid water content of the sample was computed. Berthel[7] explains the method of analysis in more detail.

C. Visual Observations

A meteorologist inside the sampling aircraft took visual observations of the larger particles (generally those over 100 μm in diameter), as well as the overall structure and density of the clouds. These were recorded on a magnetic tape, and transcribed later. Cohen[8] gives more information about these observations.

4. DATA AND METHOD OF ANALYSIS

Each aircraft flight consisted of four constant altitude passes at the 850, 700, 500, and 400 mb levels in the northeast quadrant of the storm. In combination, they provide a history of the growth and decay of a typical large-scale storm. In the present study, horizontal fluctuations in temperature and liquid water content were analyzed to determine whether or not they could provide a clue to the state of the storm.

---

6. Knollenberg, R. M. (1970) The optical array: an alternative to scattering or extinction for airborne particle size determination, J. Appl. Meteor., 9:86-103.

7. Berthel, R. (7 January 1980) A Method to Predict the Parameters of a Full Spectral Distribution From Instrumentally Truncated Data, AFGL-TR-80-0001, ERP 689, AD A085950. May be obtained through NTIS, or by writing to the author.

8. Cohen, I. D. (4 May 1981) Development of a Large-Scale Cloud System, 23-27 March 1978, AFGL-TR-81-0127, ERP 739, AD A106417. May be obtained through NTIS, or by writing to the author.

A constant averaging time of three seconds was used. Because the true air speed and the length of the path differed from one traverse to another, the maximum frequency and the frequency resolution also differed. These values are tabulated in Table 1.

Table 1. Frequency Resolution (Δf) and Maximum Frequency (f_N) in Cycles km^{-1} for Each Constant Altitude Traverse

Date	Pressure Altitude (mb)							
	850		700		500		400	
	Δf	f_N	Δf	f_N	Δf	f_N	Δf	f_N
23 March	.05	2.2	.04	1.9	.04	1.7	.03	1.5
24 March	.05	2.2	.04	2.0	.03	1.7	.03	1.5
25 March	.04	2.2	.04	1.8	.04	1.5	.03	1.3
26 March	.04	2.1	.06	2.0	.03	1.7	.04	1.5

To enhance the signal-to-noise ratio of the data, and emphasize whatever peaks are present in the fluctuation spectrum, the data were filtered to remove the effect of persistence. The filter used was

$$Z_t = X_t - \rho(X_{t-1}) \qquad (1)$$

where Z_t is the modified value, X_t and X_{t-1} are the original deviations from the mean, $\bar{X}$, at times t and t-1, and ρ is the autocorrelation coefficient between X_t and X_{t-1}. If the fluctuations about the mean vary as a Markov process, the power spectrum of the unfiltered data will be that characteristic of red noise (the power concentrated near zero cycles per kilometer), and the spectrum of the filtered data will be that of white noise (equal power across the frequency range), characteristic of random data.[9]

9. Dyer, R. M. (1971) Method for filtering meteorological data, Mon. Wea. Rev., 99:435-438.

An example of the raw data is shown in Figure 2. This trace, showing the horizontal variation in liquid water content about a mean value of .16 grams per cubic meter, was obtained at the 700 mb level (2.9 km) on 26 March 1978 (the fourth day of measurements). The 3-second autocorrelation coefficient for this unfiltered data was .92, indicating a high degree of persistence. Figure 3, which shows the autocorrelation coefficient as a function of increasing lag (expressed here as horizontal distance), confirms this. The slow rate of decay of the autocorrelation coefficient is characteristic of Markov processes. Conversely, if there were no persistence in the data, the autocorrelation coefficient would decrease linearly with increasing distance. Furthermore, the power spectrum of

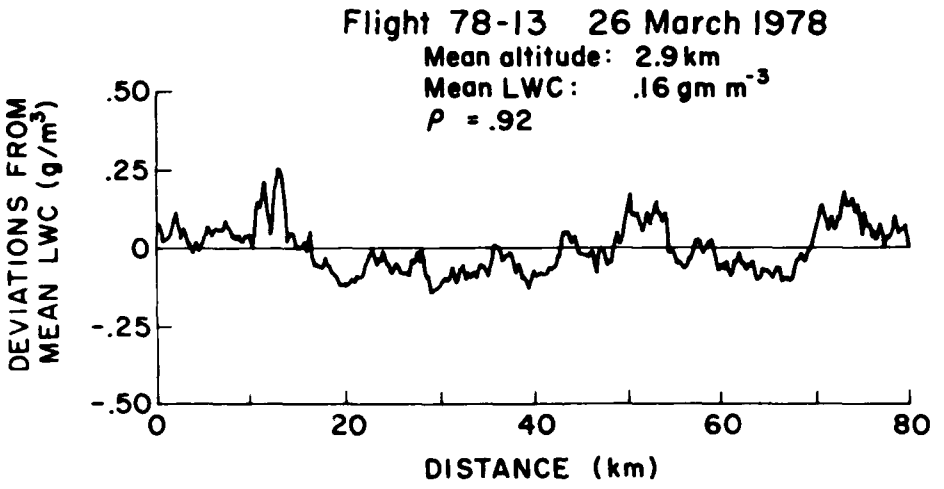

Figure 2. Deviations From Mean Liquid Water Content Measured Over a Horizontal Path at 700 mb Altitude, 26 March 1978. The autocorrelation coefficient for values 253 m apart was ρ = .92

the unfiltered data (Figure 4) shows many of the characteristics of a red noise spectrum. It is only after modifying the data using Eq. (1) that we are able to recognize the underlying periodicity in the fluctuations. The resultant power spectrum is shown in Figure 5. Note the peaks at .7, 1.1, and 1.7 cycles per kilometer. These are all significant, because they are above the level of white noise.

This method of analysis was applied to the measurements of liquid water content and temperature, at all four altitudes, for each of the four days of the field program.

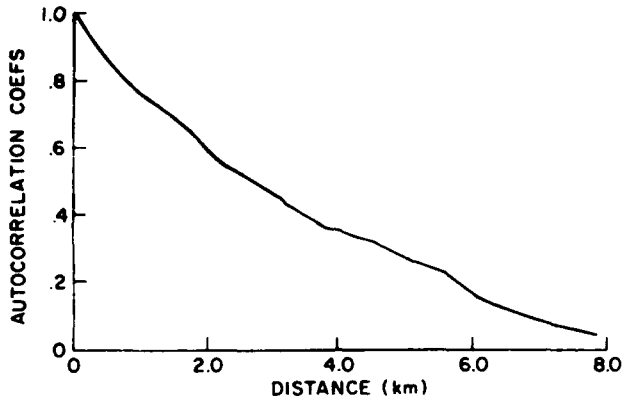

Figure 3. Autocorrelation Coefficients as a Function of Separation Distance Obtained From the Data Shown in Figure 2

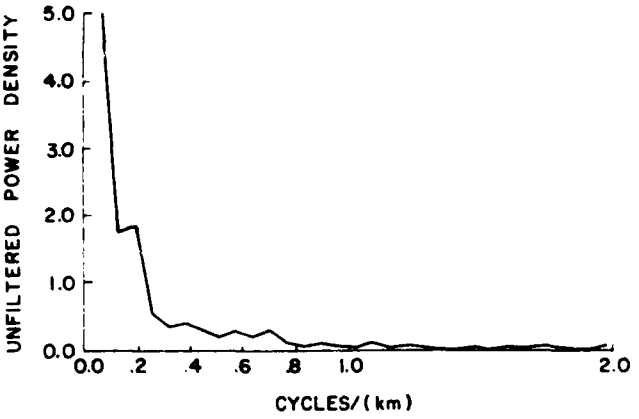

Figure 4. Power Spectrum of the Fluctuations Displayed in Figure 2, Before Filtering to Remove the Effect of Persistence

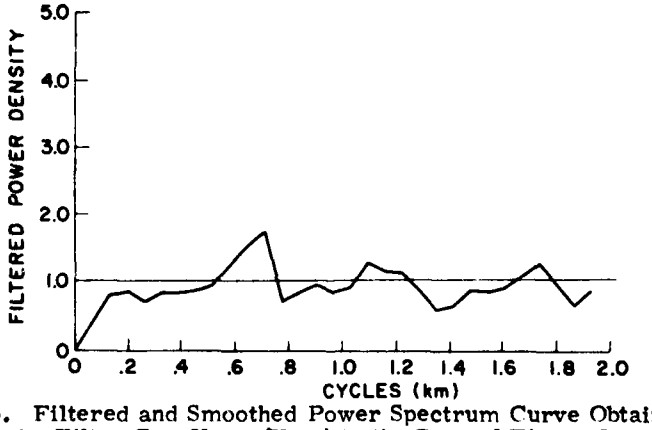

Figure 5. Filtered and Smoothed Power Spectrum Curve Obtained By Applying the Filter $Z_t = X_t - \rho(X_{t-1})$ to the Data of Figure 2

5. RESULTS AND DISCUSSION

The first statistic of interest is the autocorrelation coefficient of the unfiltered data at a lag of 3 seconds. Because of the differing aircraft speeds, a 3-second lag corresponds to a different lag distance on each of the flights. These, together with the autocorrelation coefficients, are listed in Table 2.

Table 2. Three-Second Autocorrelation Coefficients and Minimum Lag Distances

	850 mb			700 mb			500 mb			400 mb		
	D	ρ_W	ρ_T	D	ρ_W	ρ_T	D	ρ_W	ρ_T	D	ρ_W	ρ_T
23 March	232	.48	.99	257	.94	.97	298	.98	.99	327	.97	.95
24 March	230	.93	.98	255	.95	.99	300	.98	.99	340	.81	.99
25 March	232	.98	.99	277	.90	.99	326	.92	.999	382	.86	.995
26 March	234	.78	.98	253	.92	.94	302	.96	.98	339	.91	.97

D = minimum lag distance in meters

ρ_W = three-second autocorrelation coefficient of liquid water measurements

ρ_T = three-second autocorrelation coefficient of temperature measurements

In general, the lower the 3-second autocorrelation coefficient, the less the effect of the filter applied in Eq. (1). On the other hand, the lower the autocorrelation coefficient, the less the need for the filter. When the autocorrelation exceeds .99, almost all of the variance in the data is filtered out by Eq. (1). The residual may show preferred frequencies, but even the most significant of these accounts for only a small fraction of the total observed fluctuations.

The low autocorrelation coefficient at the 850 mb level on the first day (and to a lesser degree on the fourth day) is indicative of the lack of organization to be expected at lower altitudes during genesis or dissipation of a frontal system.

Table 3 lists the most significant frequency in the filtered and smoothed fluctuation spectra for each of the aircraft passes. On those occasions when there was significant power at more than one frequency, the second frequency is added in parentheses. When the power is concentrated in a frequency band, rather than

Table 3. Significant Frequencies in the Power Spectra of Temperature and Liquid Water Content Fluctuations During a Large-Scale Storm, 23-26 March 1978

	Liquid Water Content Fluctuations (cycles/kilometer)	Temperature Fluctuations (cycles/kilometer)
850 mb		
March 23	1.8 to 2.0 (1.4)	.3 (.6)
24	1.9 (1.4)	.4 (.7)
25	1.4 to 2.0	.1 (.4)
26	1.2 to 2.1	.2 to 1.0
700 mb		
March 23	1.0	.2 to .8
24	1.6 (1.0)	0 to .5
25	1.2 to 1.4	none
26	.7 (1.1 and 1.7)	.3 to 1.0
500 mb		
March 23	1.2 (.4)	none
24	.6 to 1.2	0 to 1.4
25	.2 (1.0 to 1.6)	none
26	1.3	.9 (.6)
400 mb		
March 23	.9 (.6)	.3 (1.2)
24	.9 (1.2)	.1 (.4)
25	1.3 (.7)	1.0
26	1.2	.6

at a single frequency, the range of frequencies is given. The entry "none" indicates either that the residual spectrum had no peaks above the noise level, or that the power was distributed across the entire range of frequencies measured. In the first instance, all the observed variability was explainable as persistence, resulting in a red noise power spectrum. The second situation indicates that the residual spectrum was random, that is, white noise, and contained no preferred frequencies.

On examining Tables 2 and 3, we find that the temperature fluctuations are characterized by extremely high autocorrelation coefficients, and that the spectra of the residual fluctuations after filtering show either a flat power spectrum, or a tendency for the power to be concentrated at the lowest portion of the frequency range. Both of these are indicative of persistence, with any variability behaving like a Markov process. Thus, in most cases, the temperature may be regarded as constant at a given altitude, with fluctuations smaller than the 0.1° C resolution of the instrument used to measure temperature.

Turning to the peak frequencies observed in the fluctuations of liquid water content, the frequency tends to decrease with height on a given day, and to decrease at a given altitude as the storm dissipates. It is not possible, however, to ascribe a particular frequency to a particular height and stage of the storm. The frequencies noted (between one and two cycles per kilometer) are consistent with those found by other observers as reported by Ackerman[1] and Henrion et al.[2]

The variation of liquid water content with height on each of the four days is shown in Figure 6. The existence of maximum concentrations of liquid water

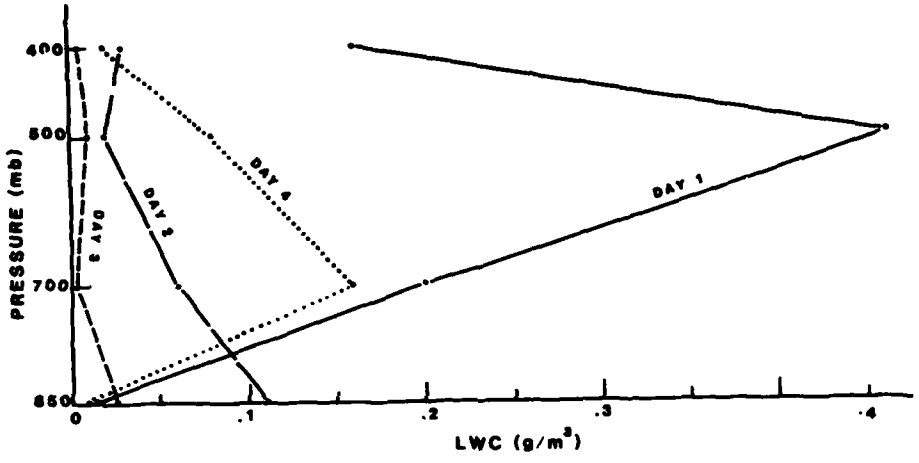

Figure 6. Vertical Distribution of Mean Liquid Water Content on 23 March (Day 1), 24 March (Day 2), 25 March (Day 3), and 26 March (Day 4)

content aloft on Days 1 and 4 are indicative of convective activity.[10] Further, the profiles show that the convection was much stronger on Day 1 than on Day 4, as evidenced by the magnitude of the maximum concentration and the height at which it occurred. This agrees with our analysis of the synoptic situation on each of the four days. Day 1 was a period during which the storm was developing and gaining strength, while on Day 4 the storm had virtually spent itself. The weak renewed convection no longer had a strong temperature contrast to draw on, and soon the storm system dissipated.

In contrast, the liquid water content decreased monotonically with height on Days 2 and 3, confirming the observation that the storm was in its mature stage

10. Hamilton, P. M. (1966) Vertical profiles of total precipitation in shower situations, J. Roy. Meteor. Soc., 92:346-366.

on those days, and most of the clouds were stratiform. Likewise, the precipitation produced by the system on Days 2 and 3 was in the form of steady rain or snow, as opposed to the showery weather seen on Day 1.

The contrast between the developing or dissipating storm, and the storm in its mature stage, is also apparent in the shapes of the fluctuation spectra (Figures 7 - 10). In Figure 7, the patterns of the temperature fluctuation spectra at 850 mb are of two types. On Days 1 and 4, there were up to four peaks spread across the frequency band. On Days 2 and 3, the peaks in the spectra were much sharper, and were concentrated below one cycle per kilometer. The spectra became steadily noisier (more fine-scale fluctuation) between Day 1 and Day 4.

Figure 8, which shows the spectra of the temperature fluctuations at the 700 mb level, shows a strikingly different spectrum on 25 March (Day 3). On that day, the residual spectrum was that of white noise. This indicates that all the temperature fluctuations at 700 mb resulted from a pure Markov process. This corresponds to a weakening in the convective activity, to the point that the cells present at the 850 mb level did not penetrate the 700 mb level.

The power spectra of the liquid water content fluctuations (Figures 9 and 10) show a grouping of spectral patterns, similar to that of the temperature fluctuation, and an increase in the spectral noise as the storm progresses. The one exception, 10(d), results from the relatively high liquid water content on Day 4 at 700 mb.

6. CONCLUSIONS

In the example presented here, variations in temperature and liquid water content along a cross section of the cloud shield of a storm give an insight into the behavior of the storm. By applying a simple filter, we have observed periodicities in the data collected along the cross section. The frequencies of these periodicities indicate the scale of the generating mechanisms involved. Clouds in convective storms will have peaks at certain frequencies; larger, stratiform clouds will have more uniform frequency distributions. The general shape of the fluctuations may indicate whether the storm is developing or dying. While these results may not apply to all other storms, they do show some possible relationships between the synoptic situation of a storm system, and the microphysics of the clouds in that system.

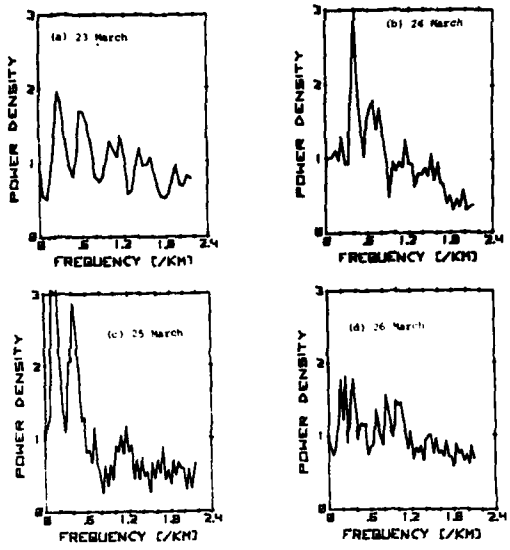

Figure 7. Filtered and Smoothed Power Spectra of Temperature Fluctuations at 850 mb for 23-26 March 1978

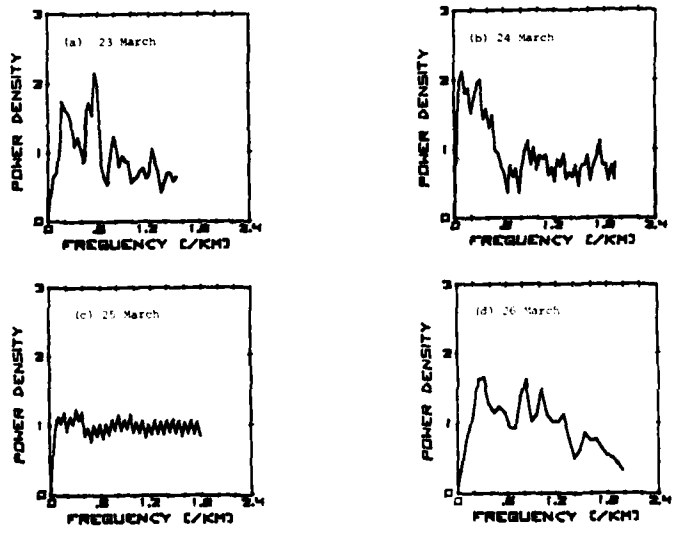

Figure 8. Filtered and Smoothed Power Spectra of Temperature Fluctuations at 700 mb for 23-26 March 1978

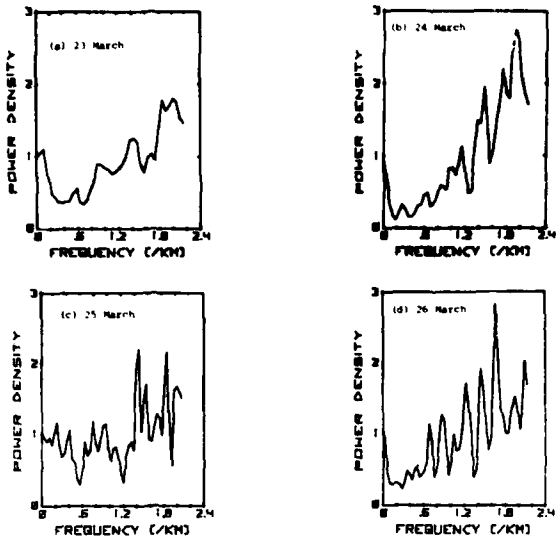

Figure 9. Filtered and Smoothed Power Spectra of Liquid Water Content Fluctuations at 850 mb for 23-26 March 1978

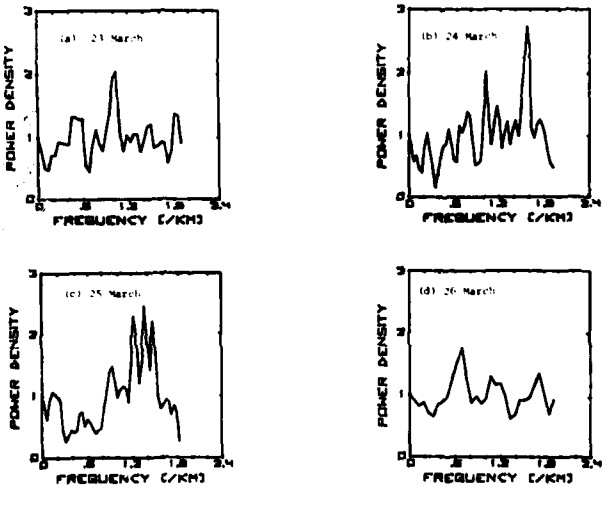

Figure 10. Filtered and Smoothed Power Spectra of Liquid Water Content Fluctuations at 700 mb for 23-26 March 1978

References

1. Ackerman, B. (1967) The nature of meteorological fluctuations in clouds, J. Appl. Meteor., 6:61-71.

2. Henrion, X., Sauvageot, H., and Ramond, D. (1978) Fine structure of precipitation and temperature in a stratocumulus cloud, J. Atmos. Sci., 35:2315-2324.

3. Foote, G. B. (1968) Variance spectrum analysis of doppler radar observations in continuous precipitation, J. Appl. Meteor., 7:459-464.

4. Dyer, R. M. (1970) Persistence in snowfall intensities measured at the ground, J. Appl. Meteor., 9:29-34.

5. Henrion, X., and Sauvageot, H. (1977) Spectral analysis of stratiform cloud radar observations. Geophys. Res. Lettrs., 4:360-362.

6. Knollenberg, R. M. (1970) The optical array: an alternative to scattering or extinction for airborne particle size determination, J. Appl. Meteor., 9:86-103.

7. Berthel, R. (1980) A Method to Predict the Parameters of a Full Spectral Distribution From Instrumentally Truncated Data, AFGL-TR-80-0001, ERP 689, AD A085950. May be obtained through NTIS, or by writing to the author.

8. Cohen, I. D. (1981) Development of a Large-Scale Cloud System, 23-27 March 1978, AFGL-TR-81-0127, ERP 739, AD A106417. May be obtained through NTIS, or by writing to the author.

9. Dyer, R. M. (1971) Method for filtering meteorological data, Mon. Wea. Rev., 99:435-438.

10. Hamilton, P. M. (1966) Vertical profiles of total precipitation in shower situations, J. Roy. Meteor. Soc., 92:346-366.

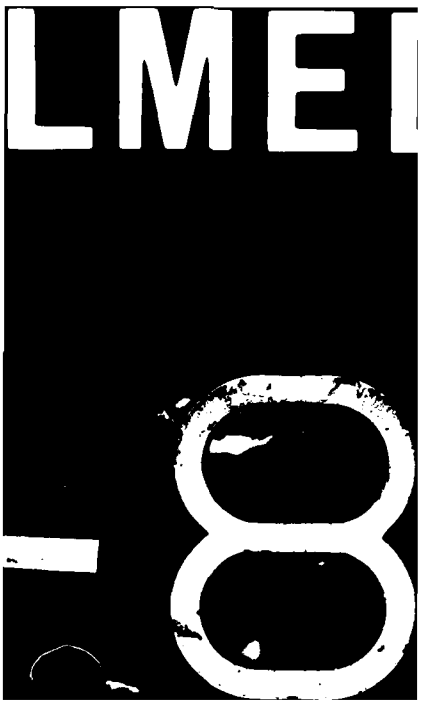
LME
8